Supporting Information for Publication

Interplay of π-stacking and inter-stacking interactions in two-component crystals of neutral closed-shell aromatic compounds: periodic DFT study.

Sona M. Melikova [a)], Alexander P. Voronin [b)], Jaroslaw Panek [c)], Nikita E. Frolov [d)], Anastasia V. Shishkina [e)], Alexey A. Rykounov [f)], Peter Yu. Tretyakov [g)], Mikhail V. Vener [*d)]

[a)] *Saint Petersburg State University, Saint Petersburg, Russia*

[b)] *G.A. Krestov Institute of Solution Chemistry of RAS, Ivanovo, Russia*

[c)] *University of Wrocław, Wrocław, Poland*

[d)] *D. Mendeleev University of Chemical Technology, Moscow, Russia*

[e)] *Northern (Arctic) Federal University, Arkhangelsk, Russia*

[f)] *FSUE "RFNC-VNIITF named after Academ. E.I. Zababakhin", Snezhinsk, Russia*

[g)] *Industrial University of Tyumen, Tyumen, Russia*

[*]*Corresponding author*: Mikhail V. Vener, e-mail: mikhail.vener@gmail.com

S1. Computational details

S1.1 Details of periodic (solid-state) DFT calculations

Tolerances on energies which control the self-consistent field convergence for geometry optimizations and frequency computations were set to 1×10^{-8} and 1×10^{-10} Hartree, respectively. The shrinking factor of the reciprocal space net was set to 3. *K*-space sampling was limited to the Γ point. Frequencies of normal modes are calculated within the harmonic approximation by numerical differentiation of the analytical gradient of the potential energy with respect to atomic position [s1].

Periodic DFT computations of molecular crystals sometimes lead to the appearance of imaginary frequencies [s2, s3, s4]. This problem is usually solved by reducing the space symmetry of the considered crystal [s2, s5]. In the present study, such procedure was applied to the crystalline $\mathbf{C_6F_6}$/naphthalene (C2/c space symmetry group [s6]) and the $\mathbf{C_{10}F_8}$/diphenylacetylene crystal (P21/n space symmetry group [s7]).

S1.2 Details of the quadrupole-quadrupole interaction calculations.

Only benzene is a strictly axially symmetric molecule (D_{6h}) among the arenes considered in this paper. The remaining molecules belong to the D_{2h} symmetry and are not formally axially symmetric. If for the measure of "axiality" we take the ratio $g = \left|Q_{xx} - \bar{Q}\right| / \bar{Q}$ - the relative deviation of Q_{xx} and Q_{yy} from their average value (for benzene $g = 0$), then the g value ranges from 3% (pyrene) to 20% (pyrene-F10) in the studied molecules (Table S1). The use of Eq. (5) for the molecules of this series is justified. The g value is 60% for diphenylacetylene $C_{14}H_{10}$; therefore, Eq. (5) can give a large error for it.

An increase in the basis set from 6-31(F+)G** to 6-311++G** weakly effects on the components of the traceless quadrupole moment (Table S3) and practically does not affect the energy of the quadrupole-quadrupole interaction (Table S3). This justifies the applicability of the PBE-D3/6-31(F+)G** level for estimating the quadrupole-quadrupole interaction energy in the considered species.

The calculations of non-periodic systems were conducted in Gaussian software in the PBE-D3/6-31+G(d,p) approximation [s8] in order to obtain the wavefunction. The non-covalent interactions were evaluated using the AIMPAC computer program suite [s9] and AIMAll software [s10].

Table S1. The traceless quadrupole moment components for a row of aromatic molecules (D*Å). The values computed at the MP2(Full)/6-311G** level are given in parentheses.

Mol. (Symm)		PBE-D3/6-31(F+)G**				PBE-D3/6-311++G**			
		X=H		X=F		X=H		X=F	
			g [a)]		*g*		*g*		*g*
C_6X_6 Benzene (D_{6h})	Q_{xx}	2.43 (3.02)	0	-2.89	0	2.77	0	-2.74	0
	Q_{yy}	2.43 (3.02)		-2.89		2.77		-2.74	
	Q_{zz}	**-4.87 (-6.05)**		**5.78**		**-5.54**		**5.47**	
$C_{10}X_8$ Naphtalene (D_{2h})	Q_{xx}	4.05 (4.91)	4.9	-4.16 (-5.10)	12.	4.38	2.8	-3.66	16.6
	Q_{yy}	3.67 (4.76)		-5.26 (-6.33)		4.14		-5.12	
	Q_{zz}	**-7.72 (-9.67)**		**9.42 (11.4)**		**-8.51**		**8.78**	
$C_{14}X_{10}$ Anthracene (D_{2h})	Q_{xx}	5.81 (6.76)	8.9	-5.51 (-7.40)	15.	6.02	4.1	-4.59	23.2
	Q_{yy}	4.86 (6.59)		-7.44 (-8.45)		5.55		-7.37	
	Q_{zz}	**-10.7 (-13.4)**		**13.0 (15.8)**		**-11.6**		**12.0**	
$C_{16}X_{10}$ Pyrene (D_{2h})	Q_{xx}	6.09 (7.48)	3.0	-6.24 (-8.00)	20.	6.46	1.1	-5.50	20.3
	Q_{yy}	5.73 (7.43)		-8.67 (-9.70)		6.32		-8.30	
	Q_{zz}	**-11.8 (-14.9)**		**14.9 (17.7)**		**-12.8**		**13.8**	
$C_{14}X_{10}$ Diphenyl-acetylene (D_{2h})	Q_{xx}	10.2 (10.1)	59.	-4.58 (-6.40)	18.	10.6	53.	-3.55	28.8
	Q_{yy}	2.66 (5.76)		-6.57 (-7.00)		3.25		-6.42	
	Q_{zz}	**-12.8 (-15.8)**		**11.2 (13.4)**		**-13.9**		**9.97**	

[a)] The measure of "axiality" $g = \frac{|Q_{xx} - \bar{Q}|}{\bar{Q}} \cdot 100,$ where $\bar{Q} = \frac{Q_{xx} + Q_{yy}}{2}$

Table S2. The traceless quadrupole moment components (D*Å) of the substituted aromatic and heterocyclic molecules, which are acceptors in two-component crystals [30].

Molecule; Refcode[a)] (Symm)		Functional/basis	
		PBE-D3/6-31G**	MP2(Full)/6-311G**
pyromellitic dianhydride; PYDMAN (D_{2h})	Q_{xx}	-16.49	-20.9
	Q_{yy}	0.98	1.00
	Q_{zz}	**15.51**	**19.9**
Tetracyanoquino-dimethane; TCYQME03 (D_{2h})	Q_{xx}	-25.32	-27.2
	Q_{yy}	4.36	5.5
	Q_{zz}	**20.96**	**21.7**

[a)] Molecule designations (the Cambridge Structural Database Refcodes).

Table S3. The distance between the centers of mass of the molecules *R* and the quadrupole-quadrupole interaction energy U_{Q1Q2}[a)] of stacked heterodimers $\mathbf{C_6F_6/C_nH_m}$ and $\mathbf{C_{10}F_8/C_nH_m}$ which structure was fully relaxed in non-periodic computations.

Heterodimer [b)]	PBE-D3/6-31(F+)G**		PBE-D3/6-311++G**	
	R, Å	U_{Q1Q2}[c)], kJ/mol	*R*, Å	U_{Q1Q2}[d)], kJ/mol
$\mathbf{C_6F_6}$/benzene	3.544	-12.86	3.562	-12.45
$\mathbf{C_6F_6}$/naphthalene	3.398	-35.53	3.398	-37.09
$\mathbf{C_6F_6}$/anthracene	3.568	-20.38	3.566	-20.76
$\mathbf{C_6F_6}$/pyrene	3.451	-43.89	3.440	-45.72
$\mathbf{C_{10}F_8}$/naphthalene	3.596	-26.44	3.550	-30.80
$\mathbf{C_{10}F_8}$/anthracene	3.411	-78.51	3.399	-80.82
$\mathbf{C_{10}F_8}$/pyrene	3.430	-84.56	3.416	-87.01

[a)] Evaluated using Eq. (6);
[b)] the abbreviations used to refer electron-deficient molecules are defined in Scheme 2;
[c)] Q_1 and Q_2 were calculated at the PBE-D3/6-31(F+)** level;
[d)] Q_1 and Q_2 were calculated at the PBE-D3/6-311++G** level.

Table S4. The values of the electron density ρ_b and its Laplacian $\nabla^2\rho_b$ at intermolecular bond critical points of crystalline naphthalene evaluated in the present study[a] vs. the literature data [s11].

Bond critical point [b], type of IMI	ρ_b, e Å^{-3}		$\nabla^2\rho_b$, e Å^{-5}	
	The present study	[93] [c]	The present study	[93]
1, H…C	0.050	0.055 0.047	0.570	0.665 0.506
2, H…H	0.039	0.051 0.036	0.504	0.592 0.418
3, H…H	0.027	0.035 0.026	0.364	0.424 0.32
4, H…H	0.025	0.032 0.024	0.312	0.387 0.278
5, H…H	0.026	0.031 0.025	0.331	0.381 0.307
6, H…C	0.029	0.03 0.028	0.334	0.378 0.309
7, H…H	0.026	0.03 0.025	0.315	0.367 0.292
8, H…C	0.021	0.023 0.02	0.238	0.284 0.217
9, H…C	0.023	0.021 0.02	0.267	0.28 0.241
10, H…H	-	0.006[d] -	-	0.067 -

[a] Computed at the PBE-D3/6-31G** level of approximation, see Subsection 2.2. The data on crystalline naphthalene (NAPHTA33) is borrowed from [s12];
[b] see Fig. S1; numbering of points is taken from Fig. 4 [s11];
[c] First line from the experimental crystal density and second line from the periodic calculation [s11];
[d] this value is too small to be determined with certainty by the existing experimental and theoretical methods [s13].

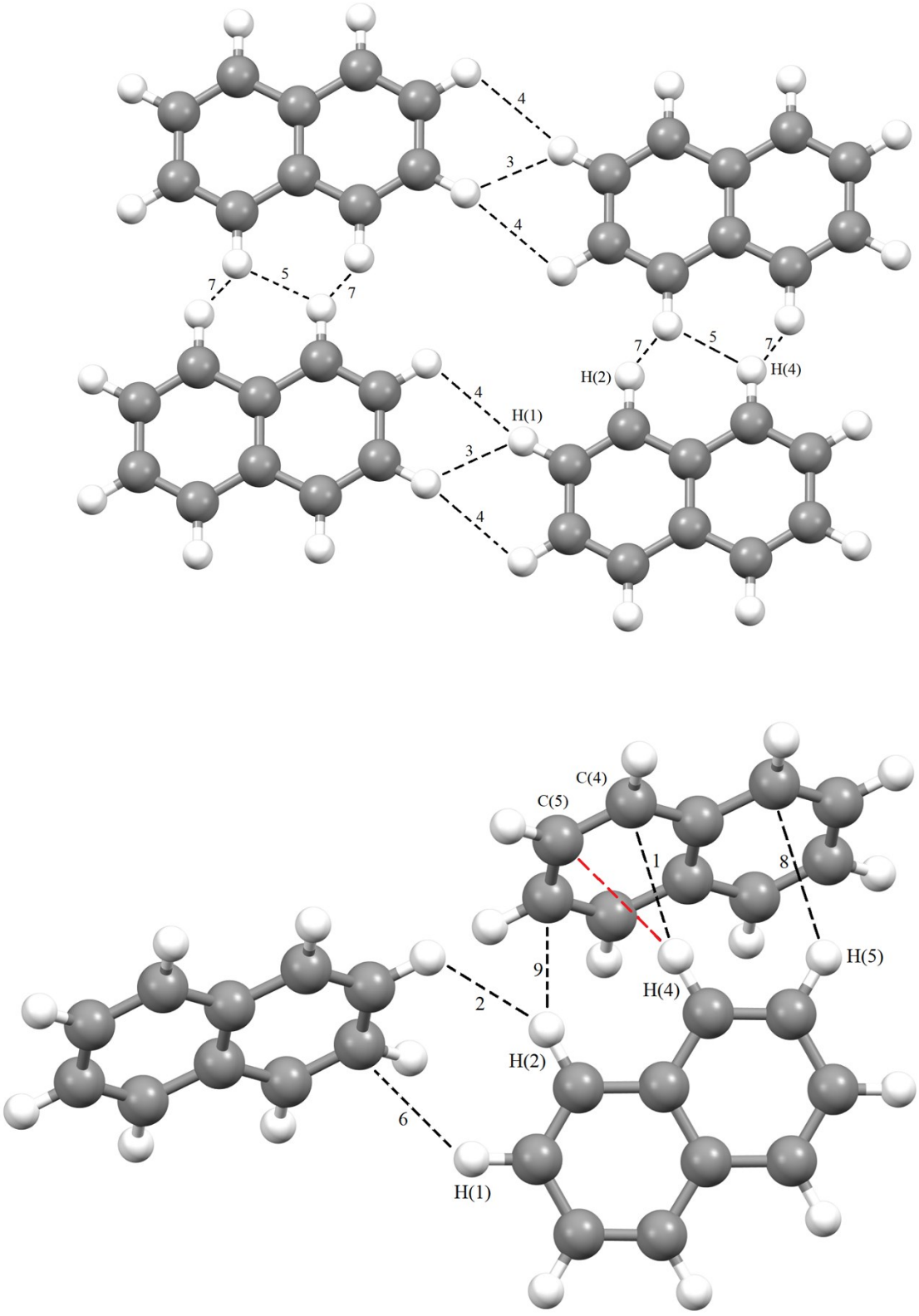

Fig. S1. IMIs in crystalline naphthalene with the corresponding bond critical points. Numbering of points is taken from Fig. 4 [s11]. For simplicity, the bond paths are given by black straight lines. H(4) atom forms two short interatomic distances with carbon atoms of the neighboring molecule (the lower panel). Bader analysis of the periodic electron density shows only one IMI, which is denoted as 1. The short C(5)…H(4) contact is given by red.

C_6F_6/ naphthalene (IVOBOK)

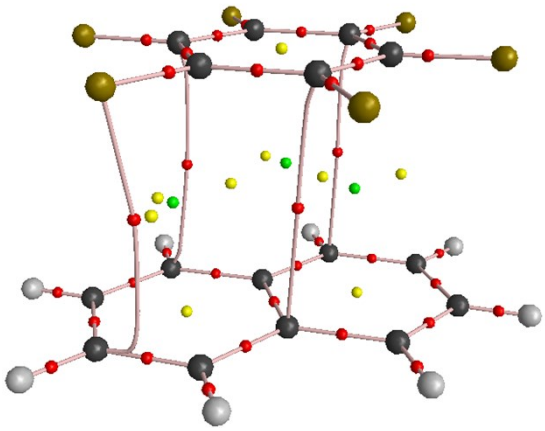

C_6F_6/pyrene (ZZZGKE)

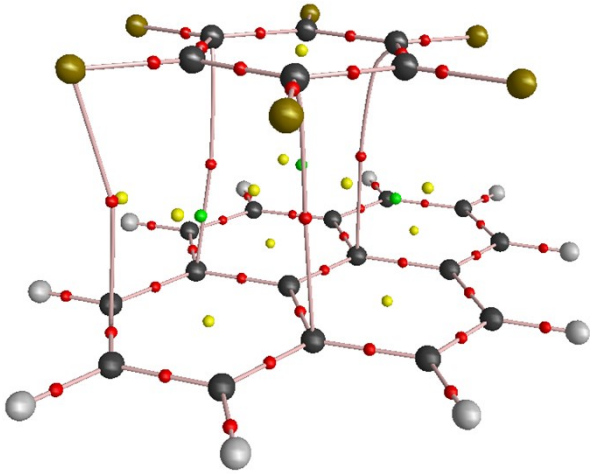

C_6F_6/anthracene (ZZZGMW)

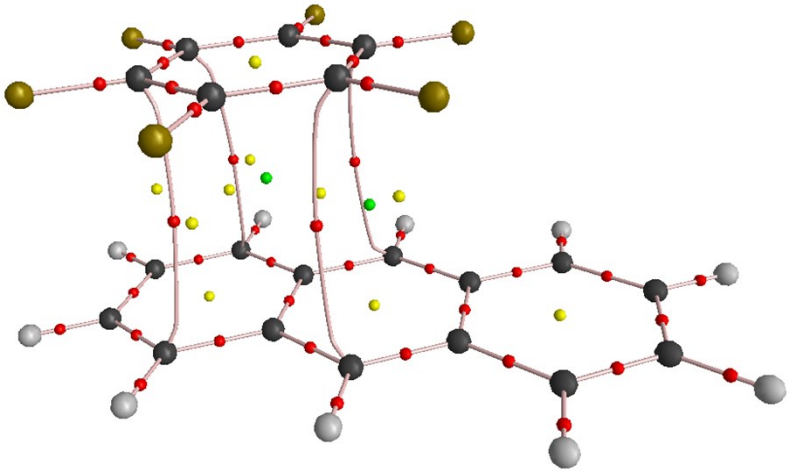

Fig. S2. The IMIs between the adjacent molecules in heterodimers, extracted from the **C_6F_6**/arene crystals. Molecule designations (the Cambridge Structural Database Refcodes) are given in parentheses. Topology of electron density [bond critical points (3,−1) are depicted as red dots, ring critical points (3, +1) as yellow, and cage critical points (3, +3) as green]

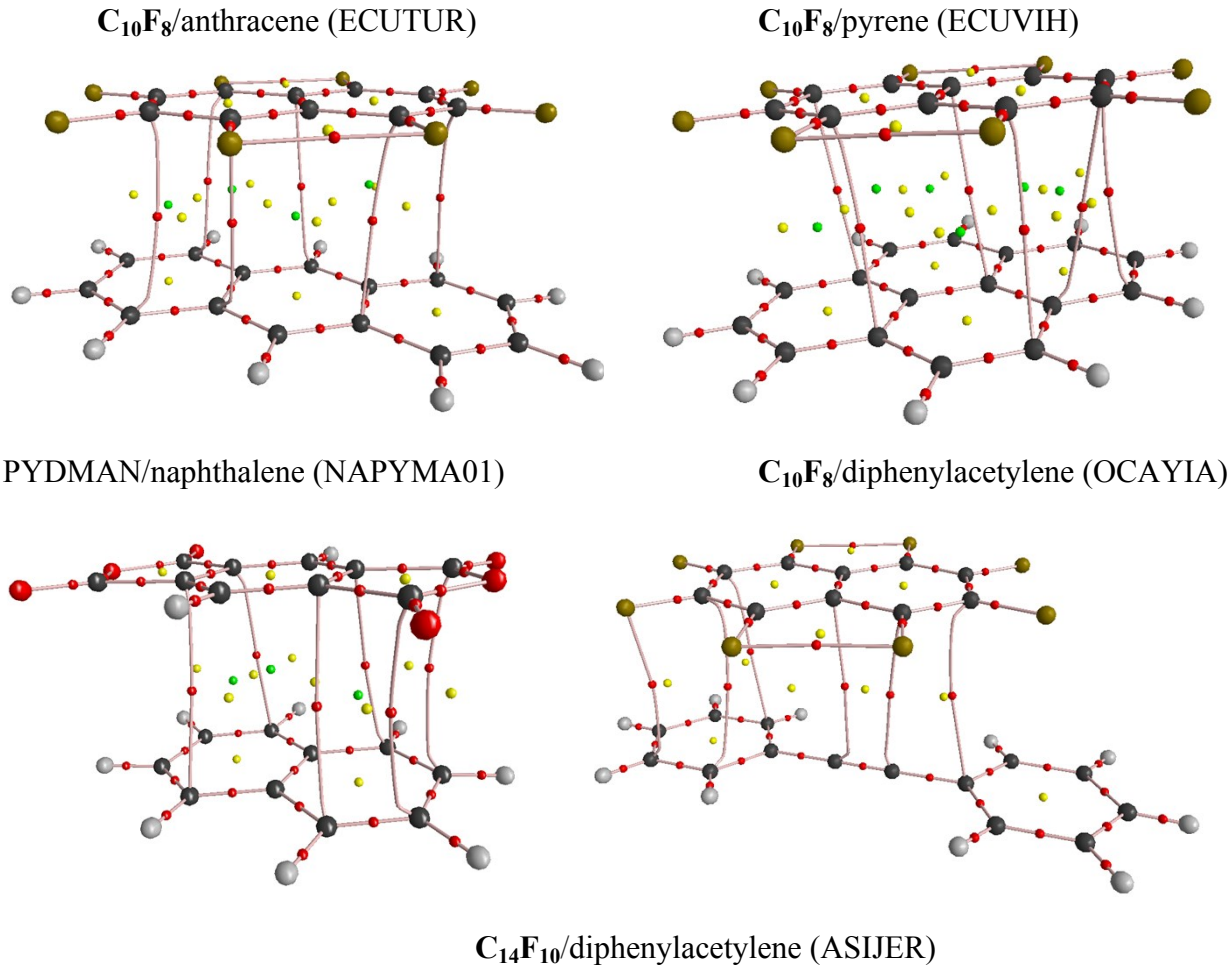

Fig. S3. The IMIs between the adjacent molecules in heterodimers, extracted from the $\mathbf{C_{10}F_8}$/arene and PYDMAN/naphthalene crystals. Molecule designations (the Cambridge Structural Database Refcodes) are given in parentheses. Topology of electron density [bond critical points (3,−1) are depicted as red dots, ring critical points (3, +1) as yellow, and cage critical points (3, +3) as green]

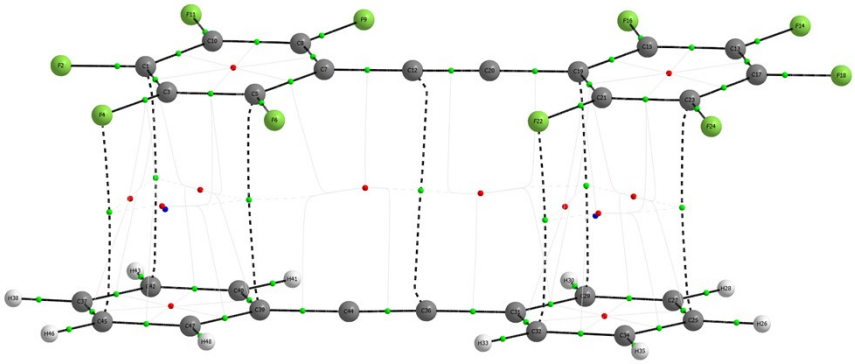

Fig. S4. The IMIs between the adjacent molecules in the heterodimer, extracted from the **$C_{14}F_{10}$**/diphenylacetylene crystal. Molecule designations (the Cambridge Structural Database Refcodes) are given in parentheses. Topology of electron density [bond critical points (3,−1) are depicted as light green dots, ring critical points (3, +1) as red, and cage critical points (3, +3) as blue]

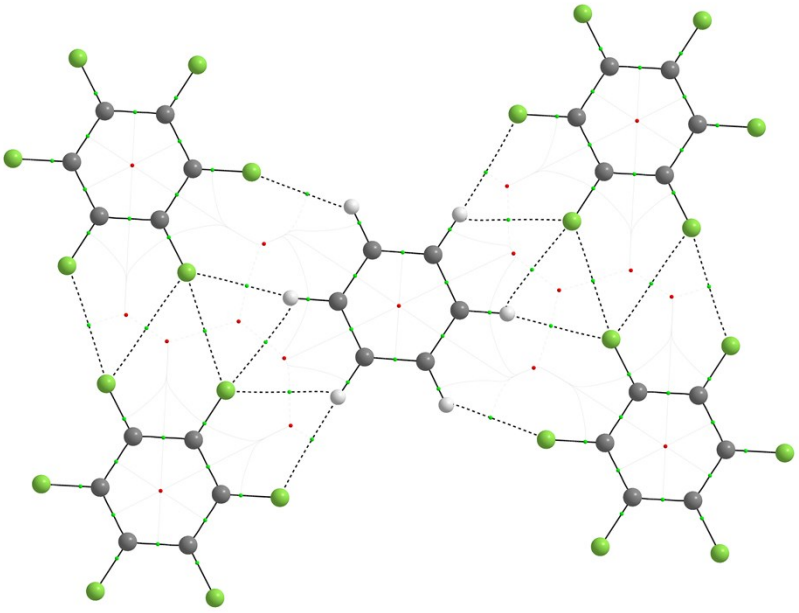

Fig. S5. Slice of crystalline **C_6F_6**/benzene along the plane of the benzene molecule. The IMIs between the adjacent molecules are given dotted lines. Topology of electron density [bond critical points (3,−1) are depicted as light green dots, and ring critical points (3, +1) as red]

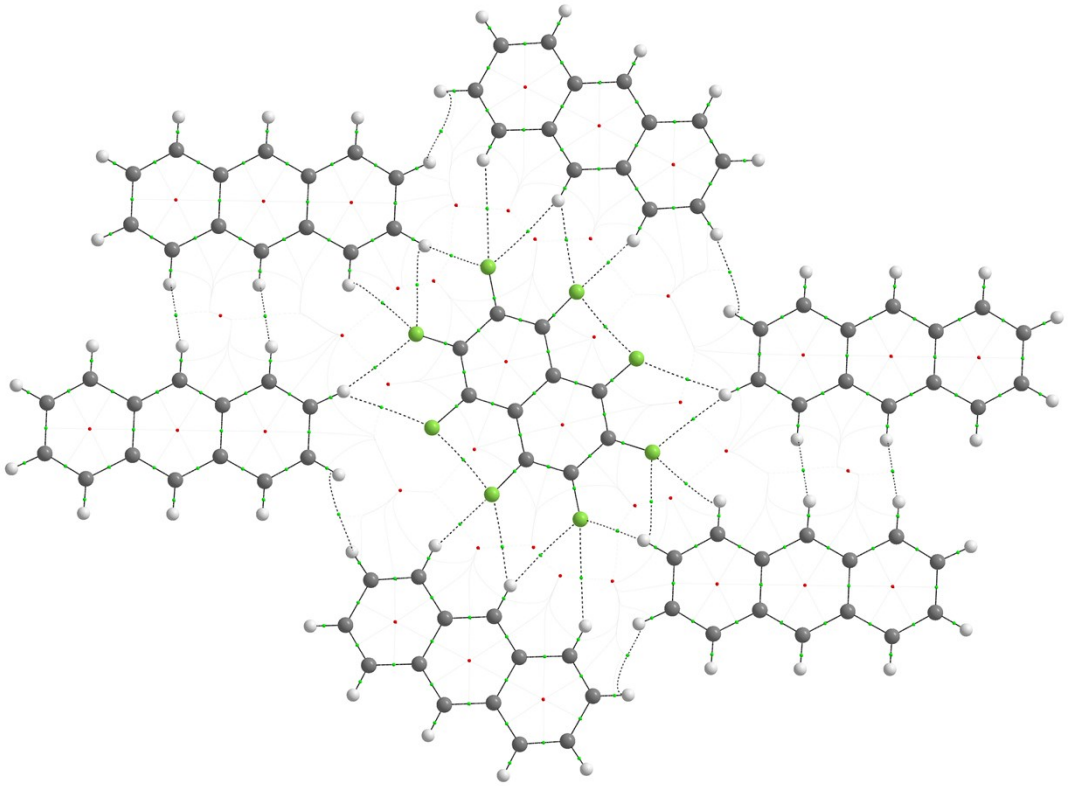

Fig. S6. Slice of crystalline $\mathbf{C_{10}F_8}$/anthracene along the plane of the $\mathbf{C_{10}F_8}$ molecule. The IMIs between the adjacent molecules are given dotted lines. Topology of electron density [bond critical points (3,−1) are depicted as light green dots, and ring critical points (3, +1) as red]

Table S5. Experimental (V_{exp}) vs. theoretical (V_{theor}) values of the unit cell volume of the considered crystals. The relative change in the volume ΔV is given in the last column.

Crystal	V_{exp}, Å^3	V_{theor}, Å^3	$\Delta V = (V_{exp} - V_{theor})/V_{exp}$ (%)
C_6F_6/benzene	527.9	542.6	-2.8
C_6F_6/naphthalene	666.6	645.5	3.2
C_6F_6/anthracene	788.7	754.9	4.3
C_6F_6/pyrene	825.1	799.0	3.2
$C_{10}F_8$/naphthalene	794.9	770.9	3.0
$C_{10}F_8$/anthracene	907.3	903.3	0.4
$C_{10}F_8$/pyrene	476.9	- [a)]	-
$C_{10}F_8$/diphenylacetylene	940.6	936.4	0.4
$C_{14}F_{10}$/diphenylacetylene	567.5	565.1	0.4
PYDMAN/naphthalene	787.1	733.4	6.8

[a)] the system did not come to stable geometry even after 500 cycles

Table S6. The interplanar distances R[a)] and the quadrupole-quadrupole interaction energy U_{Q1Q2}[b)] of homodimers of electron-deficient molecules derived from the corresponding crystal structures of perfluorinated arenes (Fig. S7).

Homodimer [c)]	R, Å	U_{Q1Q2}, kJ/mol
$(\mathbf{C_{10}F_8})_2$	5.002	-4.38
$(\mathbf{C_{14}F_{10}})_2$	5.901	-1.75
$(\mathbf{C_{12}F_8})_2$	3.982	-6.58

[a)] Distance between centers of mass;
[b)] evaluated using Eq. (5); Q_1 and Q_2 were calculated at the PBE-D3/6-31(F+)** level (Table S1);
[c)] the abbreviations used to refer electron-deficient molecules are defined in Figure S7.

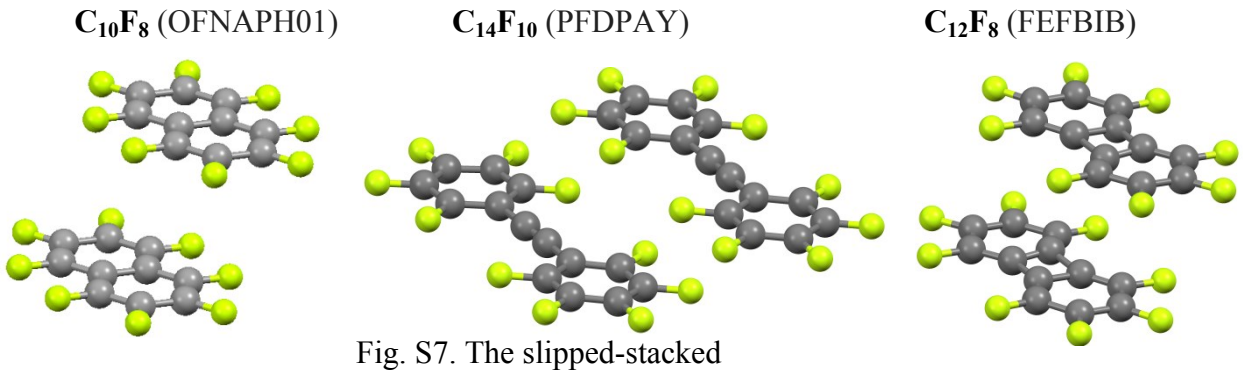

Fig. S7. The slipped-stacked configuration of the molecules in crystalline octafluoronaphthalene $\mathbf{C_{10}F_8}$ [s14], perfluorodiphenylacetylene $\mathbf{C_{14}F_{10}}$ [s15] and octafluorobiphenylene $\mathbf{C_{12}F_8}$ [s16]. Molecule designations (the Cambridge Structural Database Refcodes) are given in parentheses.

References.

s1. F. Pascale, C. M. Zicovich-Wilson, F. L. Gejo, B. Civalleri, R. Orlando, R. Dovesi, The calculation of the vibrational frequencies of crystalline compounds and its implementation in the CRYSTAL code. *J. Comput. Chem*. **2004**, *25*, 888−897.

s2. M.V. Vener, J. Sauer, Environmental effects on vibrational proton dynamics in $H_5O_2^+$: DFT study on crystalline $H_5O_2^+ClO_4^-$, *Phys. Chem. Chem. Phys.* **2005**, *7*, 258 – 263.

s3. A. V. Shishkina, A. I. Stash, B. Civalleri and V. G. Tsirelson, Electron-density and electrostatic-potential features of orthorhombic chlorine trifluoride, *Mend. Comm.* **2010**, *20*, 161–164.

s4. A. M. Reilly, A. Tkatchenko, Understanding the role of vibrations, exact exchange, and many-body van der Waals interactions in the cohesive properties of molecular crystals, *J. Chem. Phys.* **2013**, *139*, 024705.

s5. A. Sen, P. D. Mitev, A. Eriksson, K. Hermansson, H-bond and electric field correlations for water in highly hydrated crystals, *Int. J. Quant. Chem.* **2016**, *116*, 67–80.

s6. J.C. Collings, K.P. Roscoe, E.G. Robins, A.S. Batsanov, L.M. Stimson, J.A.K. Howard, S.J. Clark, T.B. Marder, Arene–perfluoroarene interactions in crystal engineering 8: structures of 1:1 complexes of hexafluorobenzene with fused-ring polyaromatic hydrocarbons *New J. Chem.* **2002**, *26*, 1740.

s7. J.C. Collings, A.S. Batsanov, J.A.K. Howard, T.B. Marder, Octafluoronaphthalene–diphenylacetylene (1/1), *Acta Cryst.* **2001**, *C57*, 870-872.

s8. Gaussian 16, Revision A.03, M. J. Frisch, G. W. Trucks, H. B. Schlegel, G. E. Scuseria, M. A. Robb, J. R. Cheeseman, G. Scalmani, V. Barone, G. A. Petersson, H. Nakatsuji, X. Li, M. Caricato, A. V. Marenich, J. Bloino, B. G. Janesko, R. Gomperts, B. Mennucci, H. P. Hratchian, J. V. Ortiz, A. F. Izmaylov, J. L. Sonnenberg, D. Williams-Young, F. Ding, F. Lipparini, F. Egidi, J. Goings, B. Peng, A. Petrone, T. Henderson, D. Ranasinghe, V. G. Zakrzewski, J. Gao, N. Rega, G. Zheng, W. Liang, M. Hada, M. Ehara, K. Toyota, R. Fukuda, J. Hasegawa, M. Ishida, T. Nakajima, Y. Honda, O. Kitao, H. Nakai, T. Vreven, K. Throssell, J. A. Montgomery, Jr., J. E. Peralta, F. Ogliaro, M. J. Bearpark, J. J. Heyd, E. N. Brothers, K. N. Kudin, V. N. Staroverov, T. A. Keith, R. Kobayashi, J. Normand, K. Raghavachari, A. P. Rendell, J. C. Burant, S. S. Iyengar, J. Tomasi, M. Cossi, J. M. Millam, M. Klene, C. Adamo, R. Cammi, J. W. Ochterski, R. L. Martin, K. Morokuma, O. Farkas, J. B. Foresman, and D. J. Fox, Gaussian, Inc., Wallingford CT, 2016.

s9. W.F. Bieger-Konig, R.F.W. Bader, T.-H. Tang, Calculation of the average properties of atoms in molecules, *J. Comput. Chem.* **1982**, *3*, 317 - 328.

s10. AIMAll (Version 19.10.12), Todd A. Keith, TK Gristmill Software, Overland Park KS, USA, 2019 (aim.tkgristmill.com)
s11. J. Oddershede, S. Larsen, Charge Density Study of Naphthalene Based on X-ray Diffraction Data at Four Different Temperatures and Theoretical Calculations, *J. Phys. Chem. A* **2004,** *108,* 1057-1063.
s12. S.C. Capelli, A. Albinati, S.A. Mason, B.T.M. Willis, Molecular Motion in Crystalline Naphthalene: Analysis of Multi-Temperature X-Ray and Neutron Diffraction Data, *J. Phys. Chem. A* **2006**, *110*, 11695-11703.
s13. V. G. Tsirelson, R. P. Ozerov, Electron Density and Bonding in Crystals; Institute of Physics Publishing: Bristol, England/Philadelphia, 1996.
s14. A. Del Pra, X-ray investigation on octafluoronaphthalene, *Acta Cryst.* **1972**, *B28*, 3438-3439.
s15. N. Goodhand, T. A. Hamor, Structures of polyfluoroaromatic compounds. V. Crystal structure of perfluorodiphenylacetylene, *Acta Cryst.* **1979**, *B35*, 704-707.
s16. J. Bowen, J.D.S. Brown, A.G. Massey, P.J. Slater, The crystal and molecular structure of octafluorobiphenylene, $C_{12}F_8$, *J. Fluor. Chem.* **1986**, *31*, 75-88.